https://doi.org/10.5194/nhess-2019-325
Preprint. Discussion started: 16 October 2019

Natural Hazards and Earth System Sciences
Discussions

Runup, Inundation, and Sediment Characteristics of December 22 2018 Indonesia Sunda Strait Tsunami

Wahyu Widiyanto[1,2], Wei-Cheng Lian[1], Shih-Chun Hsiao[1], Purwanto B. Santoso[2], Rudy T. Imananta[3]

[1]Department of Hydraulic and Ocean Engineering, National Cheng Kung University, Tainan, 701, Taiwan
[2]Department of Civil Engineering, Universitas Jenderal Soedirman, Purwokerto, 53122, Indonesia
[3]Meteorological, Climatological and Geophysical Agency (BMKG), Jakarta, 10720, Indonesia

Correspondence to: Shih-Chun Hsiao (schsiao@mail.ncku.edu.tw)

Abstract. A tsunami caused by a flank collapse of the southwest part of the Anak Krakatau volcano occurred on December 22, 2018. The affected area of the tsunami included a coastal area located at the edge of Sunda Strait, Indonesia. To gain an understanding of the tsunami event, field surveys were conducted a month after the incident. The surveys included measurements of runup height, inundation distance, tsunami direction, and sediment characteristics at 20 selected sites. The survey results revealed that the runup height and inundation distance reached 7.8 m and 292.2 m, both was found at Site Cagar Alam, part of Ujung Kulon National Park. Tsunami propagated radially from its source and arrived in coastal zone with direction was between 25° and 350° from North. Sediment samples were collected at 27 points in tsunami deposits with a sediment thickness of 1.5-12 cm. The distance of the sediment deposit area from the coast was 40%-90% of the distance of the inundation caused by the tsunami. The highest elevation of deposits was 60%-90% of the highest runup. Sand sheets were sporadic, highly variable, and highly influenced by topography. Grain sizes in the deposit area were finer than those at their sources. The sizes ranged from fine sand to boulders, with medium sand and coarse sand being dominant. All sediment samples had a well sorted distribution. An assessment of the boulder movements indicates that the tsunami runup had minimum velocities of 4.0-4.5 m/s.

Keywords: tsunami, runup, inundation, sediment, Sunda Strait, Krakatau, field survey

1 Introduction

A tsunami took place in Sunda Strait on December 22, 2018, at 22:00 Western Indonesia Time (+7 UTC). It shocked the local residents because it came without any warning signs, such as earthquake shocks. The source of the tsunami was the Anak Krakatau volcano, a sea mountain in the middle of Sunda Strait. The southwestern slope of the mountain experienced a landslide below the sea surface that resulted in the movement of sea water, which propagated to land in the form of a tsunami wave. When the tsunami reached land, its large energy caused a lot of damage and casualties. Records obtained from the Indonesian National Disaster Management Agency (Indonesian: Badan Nasional Penanggulangan Bencana, BNPB) show 430 deaths, 1015 collapsed houses, and a lot of other damage (e.g., seawalls, revetments, jetties, boats, and cars). The affected areas in Banten Province include Pandeglang and Serang Districts and those in Lampung Province include the regencies of South Lampung, Tanggamus, and Pesawaran.

Sunda Strait is home to the Krakatau (or Krakatoa) volcano. It is famous for the 1883 Krakatau eruption, which caused a 30-m tsunami that led to 36,000 fatalities and affected the Earth's climate and weather for several weeks, as reported by Verbeek (1884). The 1883 eruption of Krakatau and the resulting tsunami have been widely discussed (e.g., Yokoyama 1987; Camus *et al.* 1992; Maeno and Imamura 2011; Paris *et al.* 2014). A young volcano called Anak Krakatau (Child of Krakatau) appeared above sea level in 1929. It grew to 338 m above sea level in September 2018. This very active volcano was the source of the tsunami discussed in the present study.

https://doi.org/10.5194/nhess-2019-325
Preprint. Discussion started: 16 October 2019

Natural Hazards and Earth System Sciences
Discussions

The generation of the tsunami that occurred on December 22, 2018, in Sunda Strait was triggered by the collapse of a flank in the southwest part of the Anak Krakatau volcano. Satellite imagery shows that the area of the body of the marine volcano that was lost was 64 hectares; the collapsed volume was estimated to be 150-180 million m^3 (Kasbani, 2018). As a result of the collapse of some of the volcano's body, the volcano's height decreased from 338 to 110 m above sea level. The tsunami caused by the collapse of the Anak Krakatau flank was investigated by Giachetti et al. (2012). They used a numerical model to simulate an unstable flank collapse in the southwest part of Anak Krakatau. A hypothetical volume of 280 million m^3 produces a wave with an initial height of 43 m on Sertung, Panjang, and Rakata islands that then spreads to the beaches in the western part of Java Island, including Merak, Anyer, Carita, Panimbang, and Labuhan, and Sumatra Island, reaching Bandar Lampung City. The actual area affected by the December 22 event is consistent with their model, but different in magnitude due to the use of the worst case scenario in the simulation.

Tsunamis in Sunda Strait are of great concern because the strait is important both locally and globally. It connects the two main islands of Java and Sumatra, whose population accounts for 79% of Indonesia's population. About 6.9 million people live in the coastal area of the strait in Banten Province and Lampung Province. The strait, between Merak and Bakauheni, is the busiest inter-island crossing in Indonesia, with more than 50,000 passengers/day and more than 20,000 vehicles/day. The strait is also an international route for large ships. It is the second-most crowded waterway after Malacca Strait, with 70,000 vessels a year passing it. There are three industrial regions at the edge of the strait, namely Cilegon, Serang, and Tanggamus. There is also a special economic zone in this region, namely Tanjung Lesung. The beaches in the strait are a tourist destination. There are two UNESCO world heritage sites across from each other; one at the western tip of Java Island (Ujung Kulon National Park) and the other at the southern tip of Sumatra Island (Bukit Barisan Selatan National Park). Bandar Lampung, which has a population of 1 million, is the provincial capital and faces the strait directly. Jakarta, the capital of the Republic of Indonesia, is relatively close to the strait.

Post-tsunami field surveys were conducted to obtain data for future mitigation and development activities in the region. The surveys began exactly a month after the tsunami, January 22, and ended on January 28, 2019. Our team included people from Indonesia and Taiwan. We carried out measurements of the runup height and inundation distance of the tsunami. In addition, we also measured flow directions and sediment deposits caused by the tsunami.

2 Study Area

The tsunami has had a serious impact on life in the surrounding area. The affected area covers the coastal area on the western tip of Java Island (Banten Province) and the southern tip of Sumatra Island (Lampung Province). Banten Province covers two districts, namely Serang and Pandeglang. Lampung Province covers South Lampung Regency and the provincial capital of Lampung, namely Bandar Lampung. Post-tsunami field surveys were conducted in these areas. We selected 20 sites for observation and measurement (Table 1 and Fig. 1). These sites are located along 140 km of coast on Java Island and 80 km of coast on Sumatra Island. Sites 13 and 14 were reached by boat because of the difficult land route.

Land use at these sites includes housing, agriculture, tourism, and a national park. Sites 1, 2, 4, 7, 8, 9, and 10 (Karangsuraga, Pasauran, Pejamben, Tanjungjaya 1, and Tanjunglesung 1-3) have houses mixed with hotels, resorts, and villas. Sites 13, 15, 17, and 20 (Kertajaya Sumur, Bumi Waras, Wayurang 2, and Kunjir) have high-density housing. Sites 3, 6, 7, and 16 (Sukarame, Mekarsari, Tanjungjaya 1, and Wayurang 1) have agricultural land. Site 14 is a protected national park with limited access. Although this site has no residents, it is very important to review it because it includes the only Javan rhino (*Rhinoceros sondaicus*) habitat in the world. The Javan rhino is one of the most threatened mammals on earth, with a population of less than 100. The distribution of the rhino indicates that tsunamis are a significant risk to the species in the area (Setiawan et al., 2018).

https://doi.org/10.5194/nhess-2019-325
Preprint. Discussion started: 16 October 2019

Natural Hazards and Earth System Sciences Discussions

Each site has a different beach profile. Most sites are natural beaches. Sites 2, 4, 8, 9, and 10 (Pasauran, Pejamben, and Tanjunglesung 1-3) have coastal structures (e.g., sea walls) and sites 5, 17, and 20 (Sukamaju, Wayurang 2, and Kunjir) have revetments.

Figure 1: Locations of field surveys. Sunda Strait lies between Java Island and Sumatra Island in Indonesia. Site numbers are followed by site names. Numbers in brackets indicate inundation distances and runup heights in meters, respectively

Table 1 Field survey sites and measurements

3 Method

Measurements of runup and inundation were conducted using conservative terestrial surveying methods with optical and laser devices (e.g., total stations, handheld GPS devices, and laser distance meters). The maximum runup and inundation limits are based on remaining tsunami trail marks at measurement locations. The tracks were in the form of debris, fallen trees, plants that change color, and damage to buildings. The observed damage to buildings and structures was caused by the tsunami because there were no other causes, such as the earthquakes and liquefaction in the 2018 Sulawesi tsunami (Widiyanto et al., 2019). In addition, information regarding inundation limits and highest runup was also obtained from eyewitnesses. IOC Manuals and Guides No. 37 (1998 and 2014) and field survey reports (Maramai and Tinti 1997; Farreras 2000; Matsutomi *et al*. 2001; Fritz and Okal 2008) were used as guidelines for the implementation of this field survey.

Sediment samples were collected from selected points at measurement locations that could be in the swash zone, nearshore, berm, or deposit areas (Table 2 and Fig. 2). The measurement of deposit thickness in sandy sheets was carried out by digging a number of shallow holes. The measured thickness was considered to be near the maximum thickness. This method was qualitative and subjective because tsunami deposits are discontinuous, sporadic, and scattered over a flooded area. Sand sheets deposited on land vary greatly due to the influence of sedimentary sources and topography. A pit was made at each selected point to observe layers suspected to have been produced by the tsunami. We took only one sample at each pit for laboratory testing and did not take vertical samples at intervals of 1 cm, as done by some researchers (Gelfenbaum and Jaffe 2003; Hawkes *et al.* 2007; Srinivasalu *et al.* 2007; Srisutam and Wagner 2010), because a detailed analysis was not our focus, particularly the number of tsunami waves and the vertical variation of sediment. The grain size of the samples obtained from the field was tested using ASTM standard sieve analysis. In addition, we investigated boulder movement at four sites.

Figure 2: Aerial photographs from Google Earth of transects including highest runup point and deposit pit.

4 Runup

The runup was measured by determining the height difference between the highest point of sea water rise onto land and the coastline. Runup is influenced by the characteristics of the ground surface and slope. The measurement results from our field surveys show that runup ranged from 1 to 8 m (Table 1 and Fig. 1). A runup height of about 1 m was found in many locations, at which no damage was found. The highest runup was found at the Cagar Alam, Kunjir, and Tanjung Jaya 2 sites, with heights of 7.8, 7.7, and 7.0 m respectively. The Cagar Alam (sanctuary) site is part of the Ujung Kulon National Park. This site has a flat topography and a dense forest. The guard post and water police office were completely destroyed by the tsunami. The

https://doi.org/10.5194/nhess-2019-325
Preprint. Discussion started: 16 October 2019

Natural Hazards and Earth System Sciences
Discussions

Kunjir site, which is densely inhabited, had the second most victims after the Sumur site. This site is located on Sumatra Island about 38 km from the tsunami source. The Tanjung Jaya 2 site is a private resort with many tourists. The topography is relatively flat but suddenly rises at a distance of about 250 from the coastline due to a long hill. A large boulder moved by the tsunami was found at this site.

5 Inundation

The distance from the runup point to the coastline is defined as the inundation distance (IOC Manuals and Guides No. 37, 2014). This distance can be easily obtained using a distance measurement instrument or GPS. We used total stations for this purpose. The results of our field measurements show that the inundation distance ranged from 10 to 290 m (Table 1 and Fig. 1). The wave with an inundation distance of 10 m and a runup of 1 m at site 15 (Bumi Waras) was not felt by the population. This site was chosen to represent the area of Bandarlampung City, which is the capital of Lampung Province. This city has a population of 1 million (2018) and must thus develop tsunami mitigation strategies. The longest inundation distance was found at site 14 (292.2 m), in the sanctuary, which also had the highest runup. At this site, measurements were made near the mouth of a small river. Long inundation distances may be caused by relatively flat topography with relatively few obstacles. Tsunami may also travel faster through a stream channel. A relatively long inundation (284.2 m) was also found at Tanjungjaya 2, a site with a relatively high runup. Fortunately, not many people live around this site other than at a resort complex, which suffered severe damage.

6 Tsunami Wave Direction

The tsunami spread out from its source on the Anak Krakatau volcano to the beaches at the edge of Sunda Strait. To determine the direction of the tsunami that arrived at the beach, we obtained information from eyewitnesses. The tsunami hit at night and thus its arrival was difficult to see. Fortunately, it hit during a full moon period, so that there was some light. In addition to eyewitness accounts, we obtained evidence in the field related to the direction of the tsunami propagation. The evidence was in the form of fallen tree trunks, sloping vegetation and shrubs, damaged buildings, and building components carried away by the flow (Fig. 3).

Figure 3: Evidence of tsunami direction. Arrows show the direction of tsunami flow on the ground surfaces.

Our survey results show that the direction of the tsunami propagation was radial from the source (Fig. 4). The tsunami traveled east on the coast between Anyer and Labuhan (sites 1-6). In the vicinity of Tanjung Lesung (sites 7-13), the tsunami was directed to the southeast, and in part of Ujung Kulon National Park (Site 14), the tsunami was directed southward. The tsunami was directed to the north and slightly to the northeast on Sumatra Island (sites 15-19). The westward tsunami toward the Tanggamus area was relatively small and insignificant. We did not include this area in the survey. The smaller magnitude of the tsunami to the west is likely due to obstruction by the island of Sertung and bathymetry factors. The Anak Krakatau mountain avalanche had a southwest direction, but the tsunami in this direction had no impact on human life because it leads to the open sea (the Indian Ocean), with increasing depth from the tsunami source. Table 1 contains the quantity of tsunami wave direction arrived in coastal area. The direction ranges from 25° to 350° from north that it indicates radially propagation of the tsunami wave.

Figure 4: Direction of tsunami propagation, the tsunami spread radially from its source.

https://doi.org/10.5194/nhess-2019-325
Preprint. Discussion started: 16 October 2019

Natural Hazards and Earth System Sciences
Discussions

7 Sediment Characteristics

7.1 Tsunami Deposits

Prehistoric (paleo-) tsunamis have been identified from sediment deposits (Atwater 1992; Dawson and Shi 2000; Peters, Jaffe and Gelfenbaum 2007). Sediment deposits can be used to explain and reconstruct significant tsunami events (Dawson *et al.* 1995; Van Den Bergh *et al.* 2003). The present study attempts to describe the impact of a recent tsunami on sediment movement around the coastal area. The tsunami carried sediment from the coast inland. However, not all sites that we measured had significant sediment deposits. Only places with a sufficient source of material had clearly observable sediment deposits (Fig. 5). The survey sites used for sediment samples are shown in Fig. 2. Sediment deposits generally do not spread evenly and continuously but are separated at certain locations, which allow it to settle. Topography controls sediment deposits; for instance, there are more sediment deposits at ground surface depressions.

Figure 5: Tsunami sediment deposit, test pits were made to measure the deposit thickness.

The best location for the observation of tsunami sediment is about 50-200 m inland from the coastline (Srisutam and Wagner, 2010) or about 50-400 m inland (Moore et al., 2006), as used for the 2004 Sumatra-Andaman tsunami. In this study, the 12 deposit pits were 15-200 m (average: 93 m) from the shoreline. Four deposit pits were less than 50 m from the shoreline (11). Three of them were at sites 1, 2, and 7, respectively, due to the short inundation and beach scarp. Another was at site 13 (Kertajaya Sumur), where high-density housing blocked the sediment transport and created a deposit a short distance from the shoreline.

The interpretation of tsunami magnitude, especially runup and inundation based on tsunami deposits, is challenging (Dawson and Shi 2000). However, the relationship between deposits and runup or inundation is still not convincing because of the high variability of tsunami deposits in terms of thickness and location. Soulsby et al. (2007) proposed a mathematical model for reconstructing tsunamis runup from sedimentary characteristics. The distance for sediment deposition is related to the inundation distance for water as:

$$L_s = \frac{L_w}{1+\alpha\gamma} \quad (1)$$

where L_s is the maximum distance inland for sediment deposition, L_w is the runup limit for water, α is as shown in Eq. 2, and γ is a comparison factor between uprush time and total uprush plus backwash time.

$$\alpha = \frac{w_s T}{H} \quad (2)$$

where w_s is the settling velocity, T is a period from the time of first wetting to final drying of inundated ground, and H is the tsunami height. Fig. 6 depicts comparison among deposit pits, deposit limit and runup elevation. Deposit pits were location of sediment sample taken where significant thickness of sediment deposit were available. Deposit limit were end location of sediment deposit. From the figure, the elevations of the significant sediment deposits lie between 25% to 85% (average 54%), and the elevation of deposit limit reached 60%-90% (average: 81%) of the runup elevation. Fig. 7 shows the distance of measured sediment deposition and water runup compared to the distance of theoretical sediment deposition calculated using Eq. 1 and Eq. 2; the results are in good agreement. The distance of area with significant sediment deposits caused by the tsunami from the coast varied in the range of 15-200 m (average: 93 m) from the shoreline or 40%-90% (average: 67%) of the inundation distance.

Figure 6: Positions of deposit pits and deposit limit compared to runup elevation.

Figure 7: Positions of deposit pits and deposit limit (measured and theoretical) compared to inundation distance.

https://doi.org/10.5194/nhess-2019-325
Preprint. Discussion started: 16 October 2019

Natural Hazards and Earth System Sciences
Discussions

The sediment samples were tested for gradations in the laboratory. The results for each site are shown in Fig. 9. The sediment in the deposit areas on land is generally finer than at the sources at the beach (nearshore or swash zone). The characteristics of the sediment are discussed in Section 7.3. The sediment deposition thickness varied greatly from one point to another at the survey sites. We chose a test pit with significant thickness for sampling. The thickness was likely near the maximum sediment thickness in the area.

7.2 Boulder Movement

Coastal boulder accumulation is usually associated with high-energy events (tsunamis, hurricanes, or powerful storms). A characteristic of many tsunamis is their ability to deposit boulders across the coastal zone (Dawson andShi, 2000). Extreme storms also have the ability to deposit boulders (Morton, Gelfenbaum and Jaffe 2007; Richmond *et al.* 2010). The interpretation of boulders is difficult along coasts where both storms and tsunamis have occurred. We identified boulders moved by a tsunami wave and runup at three survey sites based on information from eyewitnesses and their physical state. Eyewitnesses said that these boulders were in new positions after the tsunami. In addition, from the physical criteria given by Morton *et al*. (2007) and Paris *et al.* (2010), it was most likely that the boulders were moved by the tsunami. At about the time of the tsunami event, a tropical cyclone called Kenanga formed in the Indian Ocean about 1400 km from Sunda Strait. Kenanga had a speed of 75 km/h and was active from December 15 to 18, 2018 (Prabowo, 2018). The influence of this cyclone was weak in the coastal zone, and thus it was unlikely to have moved the boulders.

The largest boulder, measuring 2.7 m in diameter (10.4 tons), was found at site 11 (Tanjungjaya 2), as shown in Fig. 8a. This boulder moved from its original point in the swash zone to 82 m inland. Other smaller stones were scattered around it. In Tanjunglesung (sites 8, 9, and 10), pebbles, cobbles, and small boulders (25-50 cm) were scattered up to 40 m from the coastline. At site 4, the seawall built to protect a hotel and villas was partly destroyed and moved ashore. A seawall chunk, measuring 1 m × 1 m × 4.2 m (9.5 tons), made from rubble mound and mortar moved as far as 30 m from its place of origin (Fig. 8b). Other smaller chunks also moved.

Figure 8: (a) Boulder that moved around 82 m inland and (b) an element of seawall that moved around 30 m inland.

The characteristics of the boulders moved by a tsunami can be used to estimate the associated flow velocities. For instance, the 2004 tsunami had flow velocities of 3-13 m/s. This tsunami drove a 7.7-ton calcareous boulder 200 m and an 11-ton coral boulder as far as 900 m (Paris et al., 2010). The velocity was calculated as:

$$u = \sqrt{\left(\frac{2\mu mg}{C_d A_n \rho_w}\right)} \quad (3)$$

where μ is the friction coefficient, m is the boulder mass (kg), g is the gravitational acceleration, C_d is the drag coefficient, A_n is the area of the boulder projected normal to the flow (m^2), and ρ_w is the density of sea water. The velocities were calculated to be $u \geq 4.5$ m/s and $u \geq 4.0$ m/s for the 10.4-ton (Fig. 8a) and 9.4-ton (Fig. 8b) boulders, respectively.

7.3 Sand Size Statistics

The results of sieve analysis, namely sand grain size distributions, are shown as a cumulative distribution curve of sand grain size. Fig. 9 shows the cumulative distribution curve for 12 sites. From the curve, various diameter values were determined, including d_{95}, d_{84}, d_{50}, d_{16}, and d_5. From these diameters, other statistics can be determined, namely the mean, standard deviation, skewness, and kurtosis (Table 2). The mean can be used for grain size classification. The standard deviation is a measure of range that shows the uniformity of a sand sample. A perfectly sorted sample will have sand of the same diameter, whereas poorly sorted sand will have a wide size range. Beach sand size distributions with a standard deviation of ≤ 0.5 are

https://doi.org/10.5194/nhess-2019-325
Preprint. Discussion started: 16 October 2019

Natural Hazards and Earth System Sciences Discussions

considered well sorted, and those with a standard deviation of ≥ 1 are assumed to be poorly sorted. Skewness occurs when the sand size distribution is not symmetrical. A negative skewness value indicates that the distribution is tending to the value of small phi (large grain size). Kurtosis determines the peakedness of the size distribution. The normal distribution has a kurtosis value of 0.65. If the distribution is more diffuse and wider than the normal distribution, the kurtosis value will be less than 0.65 (Dean and Dalrymple 2004).

Figure 9: Sediment grain size results from sieve analysis for various sites.

From our results, the mean values show that medium and coarse were the dominant types of sand in the sample. Very coarse sand, granular sand, and pebbles were found at the Tanjungjaya 2 and Sukarame sites. Fine and very fine sand was also identified at several sites. The range of grain sizes found in the study area depended on the available source material. Wentworth classification was used to assess the grain size. All samples had negative standard deviations, indicating that they had well sorted distributions.

Table 2 Sediment statistics and characteristics

7 of the 10 samples taken from the swash zone had negative skewness, which indicated a large phi value and an erosive tendency in the zone. The numbers of samples with positive and negative skewness were similar (7 and 6, respectively). Some deposit samples were taken at a distance of less than 50 m from the coastline, which may still be an erosive environment. The kurtosis of the tsunami sediment indicates that grain size distributions were flat to peaked distribution. Generally, the major sources of tsunami sediment are swash zones and berm/dune zone sands, where coarse to medium sands are dominant. A minor source of tsunami sediment is the shoreface, where fine to very fine sands are dominant. However, for a coastal area where the shoreface slope is mild, the major source of tsunami sediment is the shoreface. Table 2 provides kurtosis values from which distribution of sediment range from very platykurtic to very leptokurtic.

8 Conclusion

We selected 20 sites on Java Island and Sumatra Island to observe the impact of the December 2018 tsunami, which was caused by a mass movement of an Anak Krakatau volcano flank. The survey results revealed that the runup height ranged from 1 to 8 m, the inundation distance was 10 to 300 m, and the direction of the tsunami was between 25° and 350°. The highest runup (7.8 m) and the longest inundation distance (292 m) were found at site 14 (Cagar Alam), which contains a forest area, part of a national park, and a UNESCO heritage site. Sediment samples were taken from 27 points in tsunami deposits with a sediment thickness of 1.5-12 cm. The distance of area with significant sediment deposits caused by the tsunami from the coast varied in the range of 15-200 m (average: 93 m) from the shoreline or 40%-90% (average: 67%) of the inundation distance. The elevations of the significant sediment deposits reached 60%-90% (average: 81%) of the runup elevation. Sediment material larger than coarse sand (granular sand, pebbles, cobbles, and boulders) was found at several locations. The largest boulder had a diameter of 2.7 m and a weight of 10.4 tons. From the boulder movement, the tsunami velocity at the ground surface was estimated to be more than 4.5 m/s. Sand size statistics were also given in this report. The sediment grain size ranged from very fine sand to boulders, with medium sand (diameter: 0.25-0.5 mm) and coarse sand (diameter: 0.5 -1.0 mm) being dominant. All sediment samples tested in the laboratory had a well sorted distribution, indicating that the grain sizes were relatively uniform.

https://doi.org/10.5194/nhess-2019-325
Preprint. Discussion started: 16 October 2019

Natural Hazards and Earth System Sciences Discussions

Acknowledgment

This study was funded by the Ministry of Science and Technology, Taiwan, under grant MOST 107-2221-E-006-080 and the Water Resources Agency, MOEA, under grant MOEAWRA 1080412. The authors would like to thank the Geomatics Laboratory and the Soil Mechanics Laboratory at the Civil Engineering Department, Universitas Jenderal Soedirman, Purwokerto, Indonesia. We would also like to thank Ujung Kulon National Park and Tanjung Lesung Special Economic Zone for conducting surveys in their areas. We are grateful to Mr. Sumantri from Tanjunglesung Special Economic Zone and Mr. Budi from Carita Resort for accompanying the tsunami impact review and providing detailed chronological information on the tsunami, especially in Tanjunglesung and Carita Beach, respectively. We appreciate Mrs. Sanidhya Nika Purnomo for discussion on geographical information.

References

Atwater, B. F.: Geologic evidence for earthquakes during the past 2000 years along the Copalis River, southern coastal Washington, J. Geophys. Res. Solid Earth, 97(B2), 1901–1919, doi:10.1029/91jb02346, 1992.

Van DenBergh, G. D., Boer, W., DeHaas, H., VanWeering, T. C. E. and VanWijhe, R.: Shallow marine tsunami deposits in Teluk Banten (NW Java, Indonesia), generated by the 1883 Krakatau eruption, Mar. Geol., 197(1–4), 13–34, doi:10.1016/S0025-3227(03)00088-4, 2003.

Camus, G., Diament, M., Gloaguen, M., Provost, A. andVincent, P.: Emplacement of a Debris Avalanche during the 1883 eruption of Krakatau (Sunda Straits, Indonesia), GeoJournal, 28(2), 123–128, doi:10.1007/BF00177224, 1992.

Dawson, A. G. andShi, S.: Tsunami Deposits, Pure appl. Geophys, 157, 875–897, 2000.

Dawson, A. G., Hindson, R., Andrade, C., Freitas, C. and Parish, R.: Tsunami sedimentation associated with the Lisbon earthquake of 1 November AD 1755 Boca do Rio, Algarve, Portugal, The Holocene, 5(2), 209–215, 1995.

Dean, R. G. and Dalrymple, R. A.: Coastal Processes with Engineering Application, 1st ed., Cambridge University Press, Cambridge., 2004.

Farreras, S. F.: Post-tsunami field survey procedures: An outline, Nat. Hazards, 21(2–3), 207–214, doi:10.1023/A:1008049228148, 2000.

Fritz, H. M. and Okal, E. A.: Socotra Island, Yemen: Field survey of the 2004 Indian Ocean tsunami, Nat. Hazards, 46(1), 107–117, doi:10.1007/s11069-007-9185-3, 2008.

Gelfenbaum, G. andJaffe, B.: Erosion and sedimentation from the 17 July, 1998 Papua New Guinea tsunami, Pure Appl. Geophys., doi:10.1007/s00024-003-2416-y, 2003.

Giachetti, T., Paris, R., Kelfoun, K. and Ontowirjo, B.: Tsunami hazard related to a flank collapse of Anak Krakatau Volcano, Sunda Strait, Indonesia, Geol. Soc. London, Spec. Publ., 361(1), 79–90, doi:10.1144/sp361.7, 2012.

Hawkes, A. D., Bird, M., Cowie, S., Grundy-Warr, C., Horton, B. P., Shau Hwai, A. T., Law, L., Macgregor, C., Nott, J., Ong, J. E., Rigg, J., Robinson, R., Tan-Mullins, M., Sa, T. T., Yasin, Z. andAik, L. W.: Sediments deposited by the 2004 Indian Ocean Tsunami along the Malaysia–Thailand Peninsula, Mar. Geol., doi:10.1016/j.margeo.2007.02.017, 2007.

IOC Manuals and Guides No. 37: International Tsunami Survey Team (ITST) Post-Tsunami Survey Field Guide, 2nd ed., edited by D.Dominey-Howes, L.Dengler, J.Cunnen, andT.Aarup, the United Nations Educational, Scientific and Cultural Organization, Paris., 2014.

Kasbani: Pers Rilis Aktivitas Gunung Anak Krakatau, 28 Desember 2018, 2018.

Maeno, F. and Imamura, F.: Tsunami generation by a rapid entrance of pyroclastic flow into the sea during the 1883 Krakatau eruption, Indonesia, J. Geophys. Res. Solid Earth, 116(9), 1–24, doi:10.1029/2011JB008253, 2011.

Maramai, A. and Tinti, S.: The 3 June 1994 Java Tsunami: A post-event survey of the coastal effects, Nat. Hazards, doi:10.1023/A:1007957224367, 1997.

https://doi.org/10.5194/nhess-2019-325
Preprint. Discussion started: 16 October 2019

Matsutomi, H., Shuto, N., Imamura, F. andTakahashi, T.: Field survey of the 1996 Irian Jaya earthquake Tsunami in Biak Island, Nat. Hazards, 24(3), 199–212, doi:10.1023/A:1012042222880, 2001.

Moore, A., Nishimura, Y., Gelfenbaum, G., Kamataki, T. and Triyono, R.: Sedimentary deposits of the 26 December 2004 tsunami on the northwest coast of Aceh, Indonesia, Earth Planets Sp., 58, 253–258, 2006.

Morton, R. A., Gelfenbaum, G. andJaffe, B. E.: Physical criteria for distinguishing sandy tsunami and storm deposits using modern examples, Sediment. Geol., doi:10.1016/j.sedgeo.2007.01.003, 2007.

Paris, R., Fournier, J., Poizot, E., Etienne, S., Morin, J., Lavigne, F. and Wassmer, P.: Boulder and fine sediment transport and deposition by the 2004 tsunami in Lhok Nga (western Banda Aceh, Sumatra, Indonesia): A coupled offshore-onshore model, Mar. Geol., doi:10.1016/j.margeo.2009.10.011, 2010.

Paris, R., Wassmer, P., Lavigne, F., Belousov, A., Belousova, M., Iskandarsyah, Y., Benbakkar, M., Ontowirjo, B. andMazzoni, N.: Coupling eruption and tsunami records: The Krakatau 1883 case study, Indonesia, Bull. Volcanol., 76(4), 1–23, doi:10.1007/s00445-014-0814-x, 2014.

Peters, R., Jaffe, B. andGelfenbaum, G.: Distribution and sedimentary characteristics of tsunami deposits along the Cascadia margin of western North America, Sediment. Geol., doi:10.1016/j.sedgeo.2007.01.015, 2007.

Prabowo, M. R.: Siklon Tropis “Kenanga” Tumbuh di Samudra Hindia Selatan Sumatera, bmkg.go.id, 2018.

Richmond, B. M., Buckley, M., Gelfenbaum, G., Morton, R. A., Watt, S. andJaffe, B. E.: Recent storm and tsunami coarse-clast deposit characteristics, southeast Hawai‘i, Mar. Geol., doi:10.1016/j.margeo.2010.08.001, 2010.

Setiawan, R., Gerber, B. D., Rahmat, U. M., Daryan, D., Firdaus, A. Y., Haryono, M., Khairani, K. O., Kurniawan, Y., Long, B., Lyet, A., Muhiban, M., Mahmud, R., Muhtarom, A., Purastuti, E., Ramono, W. S., Subrata, D. andSunarto, S.: Preventing Global Extinction of the Javan Rhino: Tsunami Risk and Future Conservation Direction, Conserv. Lett., 11(1), doi:10.1111/conl.12366, 2018.

Srinivasalu, S., Thangadurai, N., Switzer, A. D., Ram Mohan, V. and Ayyamperumal, T.: Erosion and sedimentation in Kalpakkam (N Tamil Nadu, India) from the 26th December 2004 tsunami, Mar. Geol., doi:10.1016/j.margeo.2007.02.003, 2007.

Srisutam, C. and Wagner, J. F.: Tsunami sediment characteristics at the Thai Andaman Coast, Pure Appl. Geophys., doi:10.1007/s00024-009-0015-2, 2010.

Verbeek, R. D. M.: The Krakatoa Eruption, Nature, 10–15, 1884.

Widiyanto, W., Santoso, P. B., Hsiao, S.-C., and Imananta, R. T.: Post-event Field Survey of 28 September 2018 Sulawesi Earthquake and Tsunami, Nat. Hazards Earth Syst. Sci. Discuss., (April 2019), 1–23, doi:10.5194/nhess-2019-91, 2019.

Yokoyama, I.: A scenario of the 1883 Krakatau tsunami, J. Volcanol. Geotherm. Res., 34(1–2), 123–132, doi:10.1016/0377-0273(87)90097-7, 1987.

https://doi.org/10.5194/nhess-2019-325
Preprint. Discussion started: 16 October 2019

Natural Hazards and Earth System Sciences
Discussions

Table 1 Field survey sites and measurements

Site	Site name	Measurement time	Coordinates		Inundation distance (m)	Runup height (m)	Tsunami direction from North (°)	Sediment sample numbers
			Long. (°)	Lat. (°)				
1	Karangsuraga	25 Jan 2019	-6.148434	105.854718	84.00	4.7	82	S-01, S-02
2	Pasauran	25 Jan 2019	-6.202289	105.836179	111.00	5.8	84	S-03, S-04
3	Sukarame	24 Jan 2019	-6.261508	105.830448	204.66	4.1	93	S-05, S-06, S-07
4	Pejamben	24 Jan 2019	-6.316783	105.831298	200.80	5.0	105	-
5	Sukamaju	24 Jan 2019	-6.390917	105.825965	125.85	2.2	110	-
6	Mekarsari	25 Jan 2019	-6.520795	105.758381	123.80	2.3	115	S-08
7	Tanjungjaya 1	27 Jan 2019	-6.509201	105.673902	60.57	1.1	210	S-09, S-10
8	Tanjunglesung 1	23 Jan 2019	-6.480980	105.659513	149.54	3.4	135	S-11, S-12, S-13
9	Tanjunglesung 2	23 Jan 2019	-6.480914	105.654575	202.17	3.6	128	-
10	Tanjunglesung 3	23 Jan 2019	-6.481270	105.652097	177.06	2.4	133	S-14, S-15, S-16
11	Tanjungjaya 2	23 Jan 2019	-6.504584	105.642052	284.17	7.0	120	S-17, S-18, S-19
12	Banyuasih	23 Jan 2019	-6.600539	105.621017	170.30	2.1	142	-
13	Kertajaya Sumur	26 Jan 2019	-6.656894	105.583253	134.68	5.0	150	S-20, S-21
14	Cagar Alam	26 Jan 2019	-6.676569	105.378788	292.19	7.8	180	S-22, S-23, S-24
15	Bumi Waras	28 Jan 2019	-5.459514	105.262263	10.00	1.1	350	-
16	Wayurang 1	28 Jan 2019	-5.72307	105.582329	181.58	4.2	30	S-25, S-26, S-27
17	Wayurang 2	28 Jan 2019	-5.745806	105.587961	81.34	4.2	34	-
18	Kotaguring	28 Jan 2019	-5.800583	105.584414	29.07	2.6	25	-
19	Sukaraja	28 Jan 2019	-5.833699	105.626956	64.44	2.4	40	-
20	Kunjir	28 Jan 2019	-5.834768	105.642150	207.13	7.7	47	-

Table 2 Sediment statistics and characteristics

Sample	Date (dd/mm/yy)	Time (+8 UTC	Lat. (°S)	Long. (°E)	Village	Subdistrict	Regency	Zone	Deposit thickness (cm)	Median D_{50} (mm)	Φ_{50}	Mean	Std. Dev.	Skew-ness	Kurto-sis	Remarks
S-01	25/01/19	16:30:38	-6.148187	105.854549	Karangsuraga	Cinangka	Serang	swash zone	-	0.650	0.621	0.883	-1.368	-0.191	-0.864	coarse sand, well sorted, very platykurtic
S-02	25/01/19	16:45:44	-6.148195	105.854774	Karangsuraga	Cinangka	Serang	deposit	12	0.330	1.599	1.698	-0.698	-0.141	0.504	medium sand, well sorted, very platykurtic
S-03	25/01/19	15:02:22	-6.202145	105.835194	Pasauran	Cinangka	Serang	swash zone	-	0.200	2.322	0.007	-2.177	1.063	0.536	coarse sand, well sorted, very platykurtic
S-04	25/01/19	15:19:01	-6.201856	105.835437	Pasauran	Cinangka	Serang	deposit	3	0.500	1.000	0.652	-1.237	0.281	0.603	coarse sand, well sorted, very platykurtic
S-05	24/01/19	16:44:32	-6.260923	105.828634	Sukarame	Labuhan	Pandeglang	nearshore	-	3.000	-1.585	-1.243	-1.757	-0.195	0.463	granular, well sorted, very platykurtic
S-06	24/01/19	16:49:13	-6.261013	105.828977	Sukarame	Labuhan	Pandeglang	swash zone	-	0.500	1.000	0.921	-0.769	0.103	0.599	coarse sand, well sorted, very platykurtic
S-07	24/01/19	16:54:01	-6.261021	105.829628	Sukarame	Labuhan	Pandeglang	deposit	6.3	0.500	1.000	0.268	-1.368	0.461	0.579	coarse sand, well sorted, very platykurtic
S-08	25/01/19	18:54:59	-6.520795	105.758381	Mekarsari	Panimbang	Pandeglang	deposit	12.7	0.330	1.599	1.656	-0.740	-0.076	0.497	medium sand, well sorted, very platykurtic
S-09	27/01/19	08:34:50	-6.509219	105.674029	Tanjungjaya 1	Panimbang	Pandeglang	swash zone	-	0.240	2.059	1.994	-0.743	0.087	1.516	medium sand, well sorted, very leptokurtic
S-10	27/01/19	08:35:35	-6.509201	105.672903	Tanjungjaya 1	Panimbang	Pandeglang	deposit	2	0.650	0.621	0.128	-1.561	0.316	0.550	coarse sand, well sorted, very platykurtic
S-11	23/01/19	12:22:32	-6.479796	105.658553	Tanjunglesung 1	Panimbang	Pandeglang	swash zone	-	0.220	2.184	2.266	-0.792	-0.103	0.790	fine sand, well sorted, platykurtic
S-12	23/01/19	12:15:53	-6.480013	105.658580	Tanjunglesung 1	Panimbang	Pandeglang	deposit	3	0.170	2.556	2.791	-1.005	-0.233	0.715	fine sand, well sorted, platykurtic
S-13	23/01/19	12:32:23	-6.480799	105.659432	Tanjunglesung 1	Panimbang	Pandeglang	deposit	1.5	0.260	1.943	1.808	-0.749	0.181	1.730	medium sand, well sorted, very leptokurtic
S-14	23/01/19	10:52:19	-6.480284	105.652178	Tanjunglesung 3	Panimbang	Pandeglang	swash zone	-	0.400	1.322	1.630	-0.844	-0.365	0.722	medium sand, well sorted, very leptokurtic
S-15	23/01/19	11:04:00	-6.480438	105.652278	Tanjunglesung 3	Panimbang	Pandeglang	deposit	6.8	0.410	1.286	1.117	-0.883	0.192	1.936	medium sand, well sorted, very leptokurtic
S-16	23/01/19	11:53:24	-6.481134	105.652333	Tanjunglesung	Panimbang	Pandeglang	deposit	3.2	0.380	1.396	1.619	-0.703	-0.317	2.008	medium sand, well sorted, very leptokurtic
S-17	23/01/19	14:28:44	-6.503221	105.639871	Tanjungjaya 2	Panimbang	Pandeglang	nearshore	-	4.200	-2.070	-2.276	-1.074	0.191	0.365	pebble, well sorted, very platykurtic
S-18	23/01/19	14:38:08	-6.502949	105.640477	Tanjungjaya 2	Panimbang	Pandeglang	swash zone	-	1.200	-0.263	-0.026	-1.460	-0.163	0.332	very coarse sand,well sorted,very platykurtic
S-19	23/01/19	14:51:05	-6.504377	105.641338	Tanjungjaya 2	Panimbang	Pandeglang	deposit	-	0.380	1.396	1.429	-0.893	-0.037	0.588	medium sand, well sorted, very platykurtic
S-20	26/01/19	18:40:59	-6.655898	105.583705	Kertajaya	Sumur	Pandeglang	swash zone	-	0.950	0.074	0.465	-1.272	-0.037	0.778	coarse sand, well sorted, platykurtic
S-21	26/01/19	14:42:08	-6.656034	105.583687	Kertajaya	Sumur	Pandeglang	deposit	2	0.220	2.184	1.826	-0.911	0.393	1.131	medium sand, well sorted, leptokurtic
S-22	26/01/19	12:27:00	-6.673185	105.379727	Cagar Alam	Sumur	Pandeglang	nearshore	-	0.220	2.184	1.800	-0.937	0.410	1.654	medium sand, well sorted, very leptokurtic
S-23	26/01/19	13:14:17	-6.674877	105.379122	Cagar Alam	Sumur	Pandeglang	swash zone	-	0.380	1.396	1.494	-0.828	-0.119	1.071	medium sand, well sorted, mesokurtic
S-24	26/01/19	14:03:24	-6.675483	105.378968	Cagar alam	Sumur	Pandeglang	deposit	7.5	0.120	3.059	3.020	-0.624	0.063	0.861	very fine sand, well sorted, platykurtic
S-25	28/01/19	14:04:46	-5.724157	105.581636	Wayurang	Kalianda	S. Lampung	nearshore	-	0.190	2.396	2.370	-0.814	0.031	0.697	fine sand, well sorted, platykurtic
S-26	28/01/19	13:48:51	-5.723089	105.581996	Wayurang	Kalianda	S. Lampung	swash zone	-	0.190	2.396	2.398	-0.660	-0.003	0.995	fine sand, well sorted, mesokurtic
S-27	28/01/19	14:04:46	-5.724157	105.581636	Wayurang	Kalianda	S. Lampung	deposit	12.3	0.170	2.556	2.959	-0.930	-1.718	-2.248	coarse sand, well sorted, very platykurtic

https://doi.org/10.5194/nhess-2019-325
Preprint. Discussion started: 16 October 2019

Natural Hazards and Earth System Sciences
Discussions
Open Access
EGU

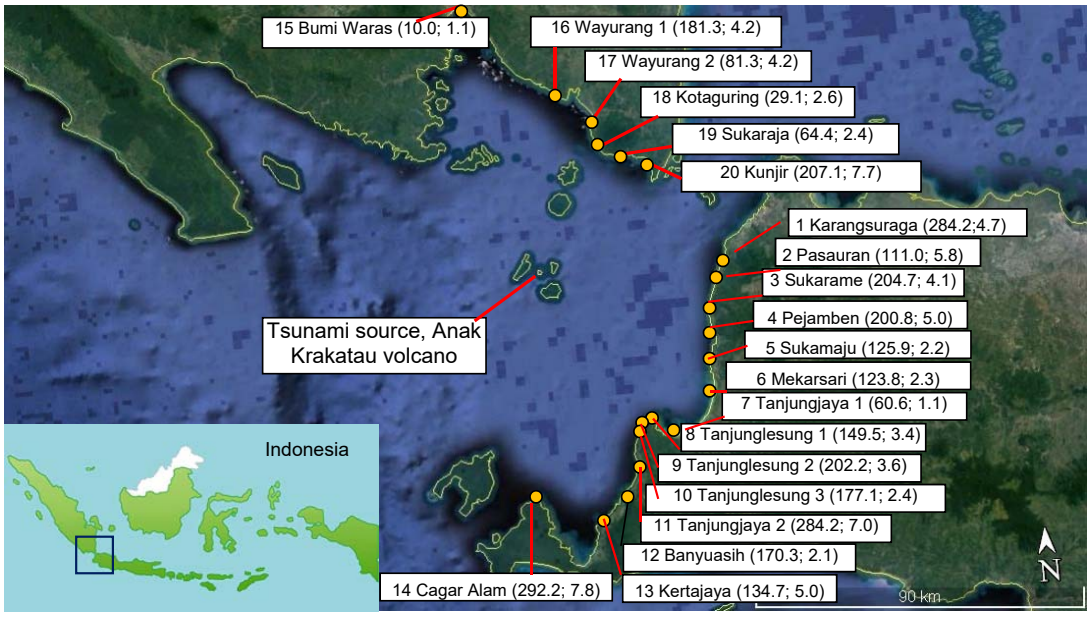

Figure 1: Locations of field surveys. Sunda Strait lies between Java Island and Sumatra Island in Indonesia. Site numbers are followed by site names. Numbers in brackets indicate inundation distances and runup heights in meters, respectively.

https://doi.org/10.5194/nhess-2019-325
Preprint. Discussion started: 16 October 2019

Natural Hazards and Earth System Sciences
Discussions
Open Access
EGU

https://doi.org/10.5194/nhess-2019-325
Preprint. Discussion started: 16 October 2019

Natural Hazards and Earth System Sciences
Discussions
Open Access
EGU

Figure 2: Aerial photographs from Google Earth of transects including highest runup point and deposit pit. © Google Earth.

https://doi.org/10.5194/nhess-2019-325
Preprint. Discussion started: 16 October 2019

Natural Hazards and Earth System Sciences
Discussions

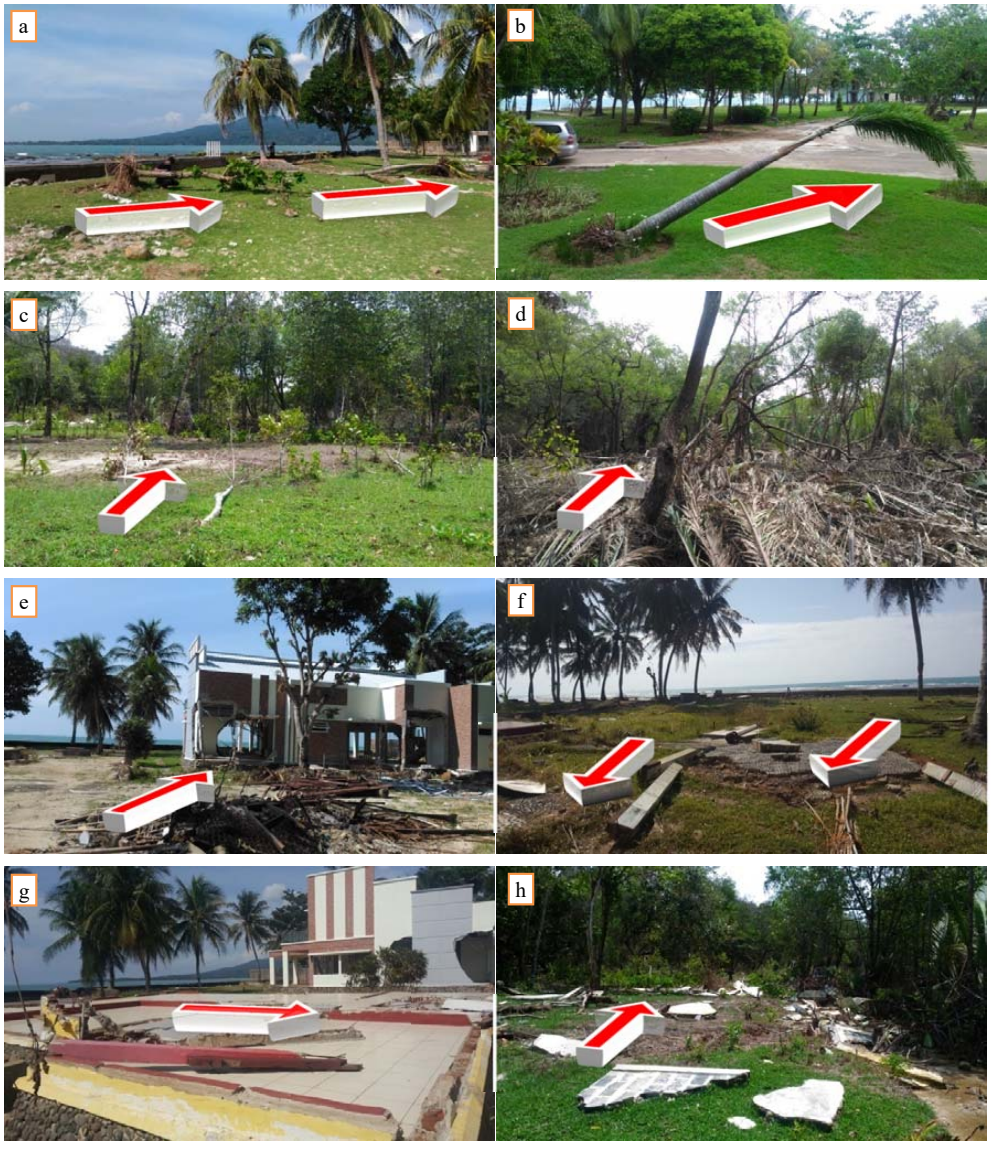

Figure 3: Evidence of tsunami direction. Arrows show the direction of tsunami flow on the ground surfaces.

https://doi.org/10.5194/nhess-2019-325
Preprint. Discussion started: 16 October 2019

Natural Hazards and Earth System Sciences
Discussions
Open Access
EGU

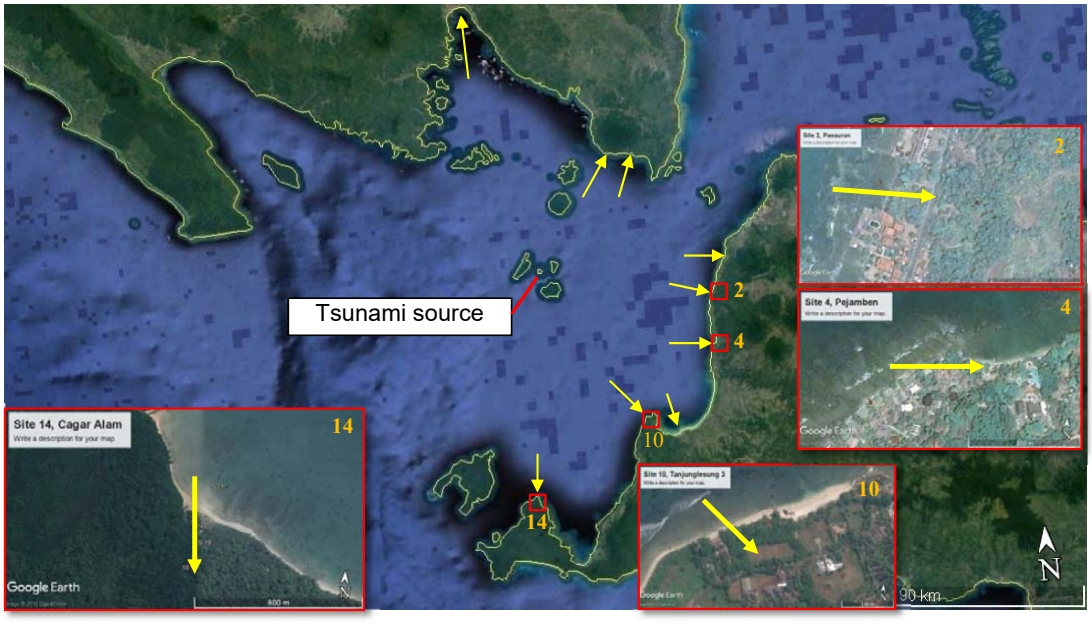

Figure 4: Direction of tsunami propagation, the tsunami spread radially from its source. © Google Earth.

Figure 5: Tsunami sediment deposit, test pits were made to measure the deposit thickness.

https://doi.org/10.5194/nhess-2019-325
Preprint. Discussion started: 16 October 2019

Natural Hazards and Earth System Sciences
Discussions

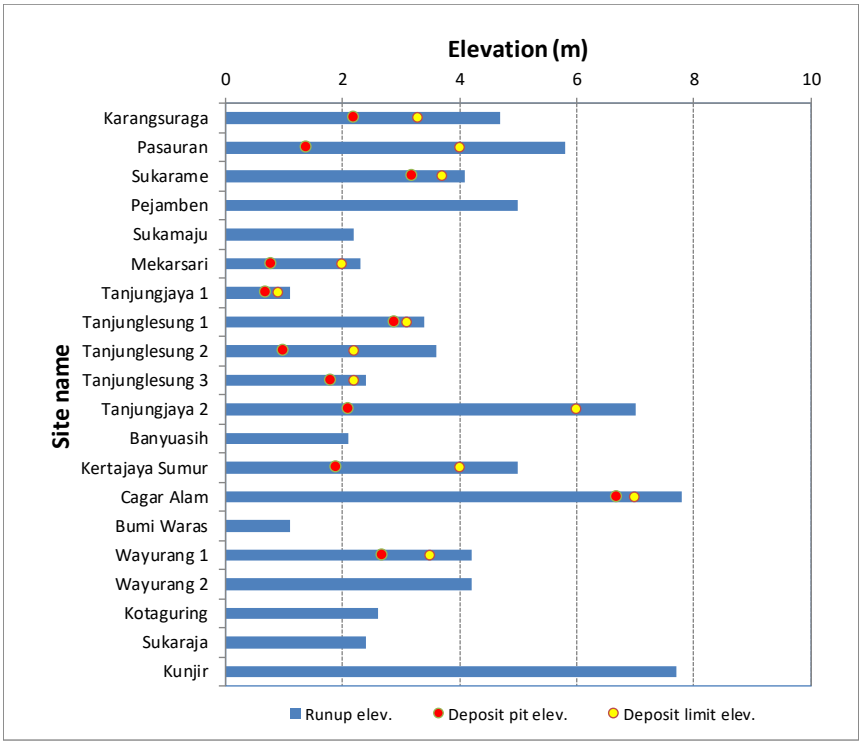

Figure 6: Positions of deposit pits and deposit limit compared to runup elevation

5

https://doi.org/10.5194/nhess-2019-325
Preprint. Discussion started: 16 October 2019

Natural Hazards and Earth System Sciences
Discussions

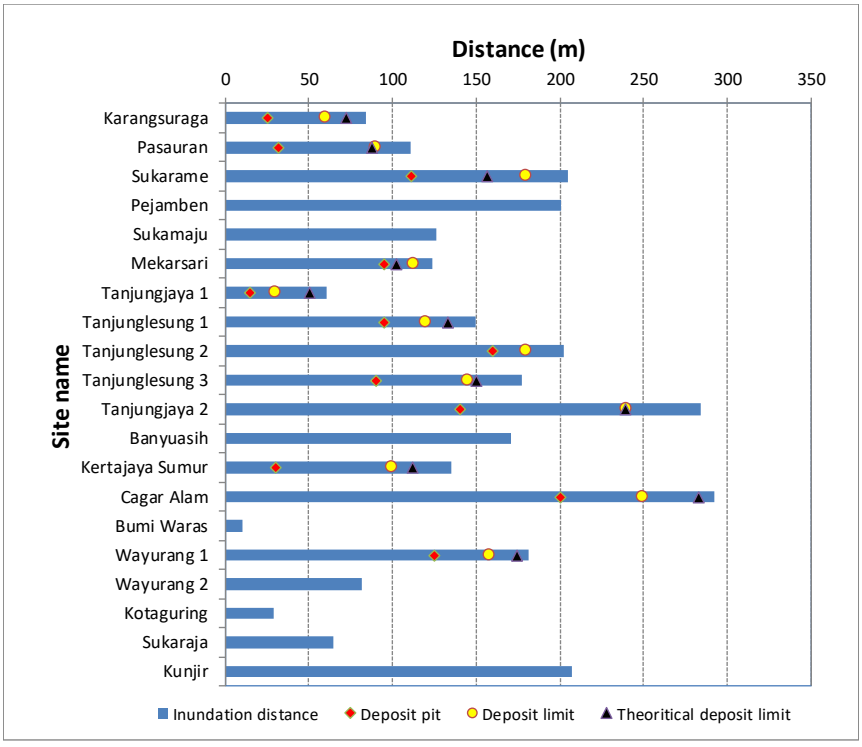

Figure 7: Positions of deposit pits and deposit limit (measured and theoretical) compared to inundation distance.

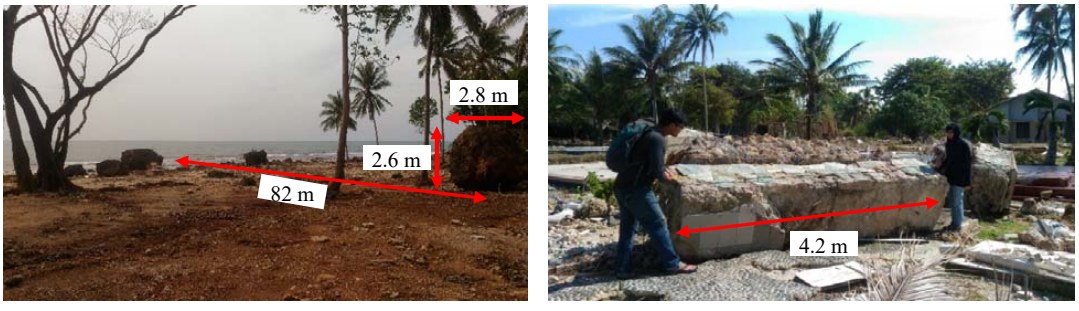

(a) **(b)**

Figure 8: (a) Boulder that moved around 82 m inland and **(b)** an element of seawall that moved around 30 m inland.

https://doi.org/10.5194/nhess-2019-325
Preprint. Discussion started: 16 October 2019

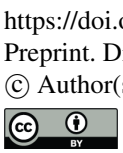

Natural Hazards and Earth System Sciences
Discussions
Open Access
EGU

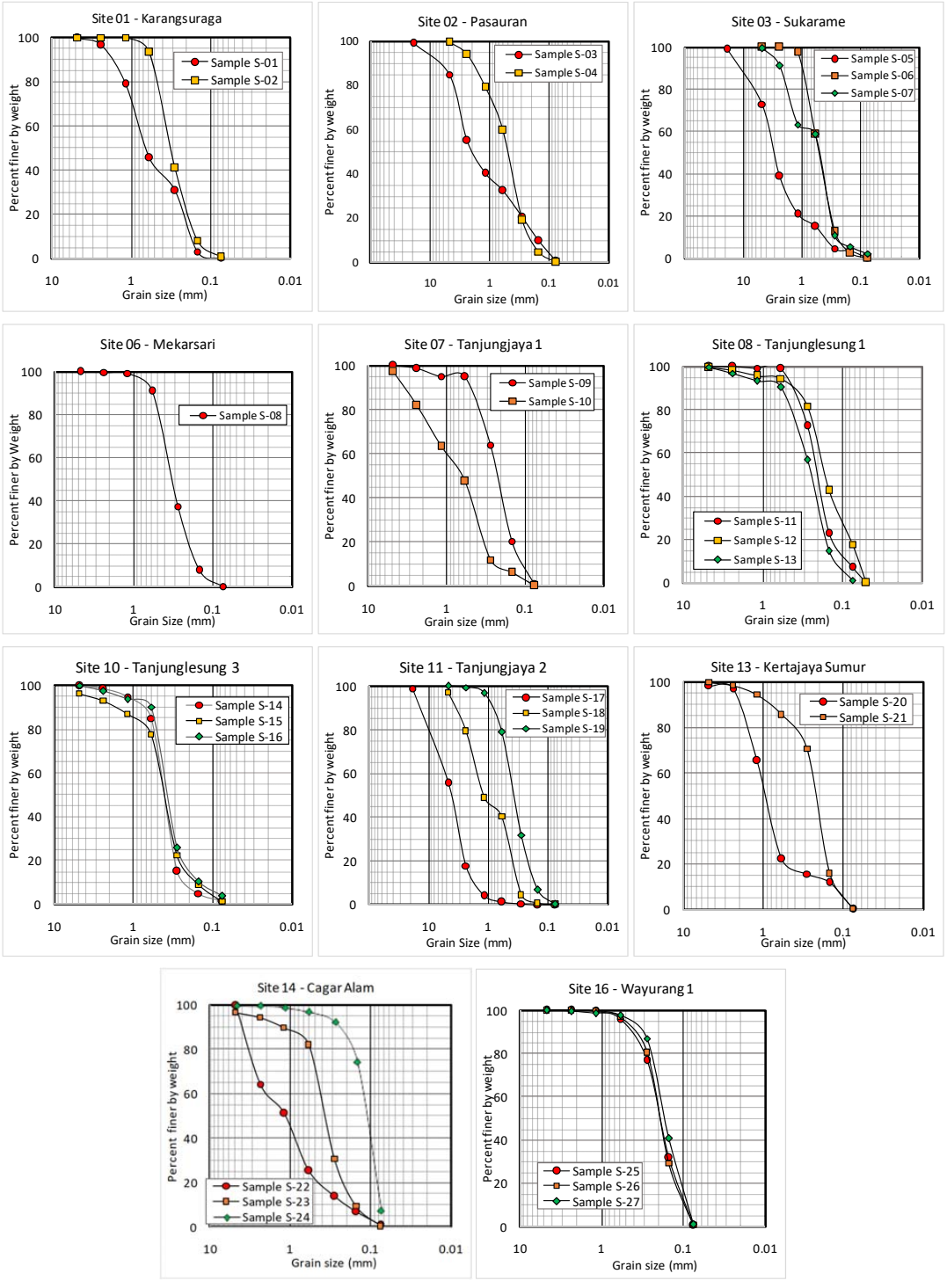

Figure 9: Sediment grain size results from sieve analysis for various sites.